

PII: S1567-5394(19)30624-3
 DOI: <https://doi.org/10.1016/j.bioelechem.2019.107449>
 Reference: BIOJEC 107449

Received Date: 9 September 2019
Revised Date: 17 December 2019
Accepted Date: 17 December 2019

This is a PDF file of an article that has undergone enhancements after acceptance, such as the addition of a cover page and metadata, and formatting for readability, but it is not yet the definitive version of record. This version will undergo additional copyediting, typesetting and review before it is published in its final form, but we are providing this version to give early visibility of the article. Please note that, during the production process, errors may be discovered which could affect the content, and all legal disclaimers that apply to the journal pertain.

Luminal addition of non-permeant Eu^{3+} interferes with luminal Ca^{2+} regulation of the cardiac ryanodine receptor

Jana Gaburjakova^{a,1}, Janos Almassy^{b,2}, Marta Gaburjakova^{a,*}

^aInstitute of Molecular Physiology and Genetics, Centre of Biosciences, Slovak Academy of Sciences, Dubravska cesta 9, 840 05 Bratislava, Slovak Republic

^bDepartment of Physiology, Faculty of Medicine, University of Debrecen, PO Box 400, Debrecen 4002, Hungary

¹ jana.gaburjakova@savba.sk

² almassy.janos@med.unideb.hu

* Marta Gaburjakova, Ph.D.
Institute of Molecular Physiology and Genetics
Centre of Biosciences
Slovak Academy of Sciences
Dubravska cesta 9
840 05 Bratislava
Slovak Republic
Tel: ++421-2-32295521
e-mail: marta.gaburjakova@savba.sk

ABSTRACT

Dysregulation of the cardiac ryanodine receptor (RYR2) by luminal Ca^{2+} has been implicated in a life-threatening, stress-induced arrhythmogenic disease. The mechanism of luminal Ca^{2+} -mediated RYR2 regulation is under debate, and it has been attributed to Ca^{2+} binding on the cytosolic face (the Ca^{2+} feedthrough mechanism) and/or the luminal face of the RYR2 channel (the true luminal mechanism). The molecular nature and location of the luminal Ca^{2+} site is unclear. At the single-channel level, we directly probed the RYR2 luminal face by Eu^{3+} , considering the non-permeant nature of trivalent cations and their high binding affinities for Ca^{2+} sites. Without affecting essential determinants of the Ca^{2+} feedthrough mechanism, we found that luminal Eu^{3+} competitively antagonized the activation effect of luminal Ca^{2+} on RYR2 responsiveness to cytosolic caffeine, and no appreciable effect was observed for luminal Ba^{2+} (mimicking the absence of luminal Ca^{2+}). Importantly, luminal Eu^{3+} caused no changes in RYR2 gating. Our results indicate that two distinct Ca^{2+} sites (available for luminal Ca^{2+} even when the channel is closed) are likely involved in the true luminal mechanism. One site facing the lumen regulates channel responsiveness to caffeine, while the other site, presumably positioned in the channel pore, governs the gating behavior.

Keywords: cardiac muscle • ryanodine receptor • luminal Ca^{2+} regulation • luminal Eu^{3+} • caffeine • planar lipid membrane

1. INTRODUCTION

In cardiac muscle, the ryanodine receptor (RYR2) functions as a Ca^{2+} release channel in the sarcoplasmic reticulum (SR) and plays a pivotal role in Ca^{2+} cycling, which is implicated in rhythmic muscle contraction [1-3]. Defective function of the RYR2 channel gives rise to various cardiac disease states, including heart failure [4-7] and familial catecholaminergic polymorphic ventricular tachycardia (CPVT), which is a life-threatening, stress-induced arrhythmogenic disease [8]. It is evident that RYR2 function must be tightly regulated to accomplish the efficient control of cardiac muscle contractility. With each heartbeat, the RYR2 channel is transiently activated by Ca^{2+} ions entering the cell via the plasmalemmal voltage-sensitive L-type Ca^{2+} channel. This mechanism is known as Ca^{2+} -induced Ca^{2+} release [9-11]. Several functional (reviewed in [12]) and the recent cryo-electron microscopy structural studies [13-15] have been aimed at understanding the three-dimensional (3D) localization of the Ca^{2+} site within the huge cytosolic assembly of a skeletal muscle isoform of the RYR channel (RYR1). Interestingly, this Ca^{2+} site is situated at the bottom of the cytosolic domain, close to the minor membrane assembly of “mushroom-like” protein. Because the RYR1 and RYR2 isoforms share a high level of sequence similarity in this region, it is reasonable to predict the same location for the cytosolic Ca^{2+} site in the RYR2 isoform [13-15].

Over the past 20 years, a substantial body of evidence has suggested a functional role for luminal Ca^{2+} (inside the SR lumen) in RYR2 regulation (reviewed in [16-19]). Currently, this regulatory pathway is considered important for Ca^{2+} signaling in cardiac muscle cells and is evidently impaired in diseased states, such as CPVT disorder [8,20] and heart failure [21-23]. The molecular mechanism underlying luminal Ca^{2+} sensing of the RYR2 channel is still not fully understood because the collective findings and their interpretations remain controversial. According to two proposed models, namely the true luminal model (Ca^{2+} binding on the luminal face) [24,25] and the Ca^{2+} feedthrough model (Ca^{2+} permeation via the channel pore to the cytosolic Ca^{2+} site) [26,27], both RYR2 faces could be involved, separately or in combination [28,29]. Whereas the presence of the cytosolic Ca^{2+} site has been widely demonstrated at the functional level and recently at the structural level, the existence and molecular identity of a luminal-facing Ca^{2+} sensor is under extensive debate. Initially, calsequestrin (CSQ2), the major Ca^{2+} -binding protein in the SR in adult cardiac muscle [30,31], was believed to transmit Ca^{2+} signals from the SR lumen to the RYR2 channel [32-35]. How exactly CSQ2 plays this regulatory role has yet to be defined, although a direct functional interaction between CSQ2 and the RYR2 channel is one possible mechanism [36]. In addition, the ability of CSQ2 to keep enough Ca^{2+} ions in close proximity to the channel pore for prompt release and/or channel activation should not be underestimated [37,38]. In support of this latter hypothesis, an intrinsic luminal Ca^{2+} site operating on the RYR2 luminal face has been proposed [34,39] and might be locally controlled by Ca^{2+} ions supplied by the attached CSQ2 [36]. Over the last five years, substantial progress has been made with respect to identification of this RYR2-resident luminal Ca^{2+} sensor. Chen et al. [8] highlighted four amino acid residues of the mouse RYR2 channel (E4872, D4875, E4878, and Q4879) that form a putative site for luminal Ca^{2+} coordination. Surprisingly, the recent near-atomic 3D structure positioned these residues in a region of the channel gate that is evidently exposed to cytosol [14,40]. Thus, the residues will not be supplied with luminal Ca^{2+} emanating from the channel pore in the lumen-to-cytosol direction when the channel gate is closed. A similar situation occurs at the cytosolic Ca^{2+} site that mediates the Ca^{2+} feedthrough mechanism. Importantly, this scenario contrasts with the principal attribute of the true luminal mechanism, where the properties of the RYR2 channel in the closed state are substantially modified by luminal Ca^{2+} [8,26,39,41-44]. Although, a proposed pathway might be relevant, it would not provide a clear picture of the luminal Ca^{2+} sensor of the RYR2

channel. Because it has also been reported that luminal Ca^{2+} regulation was completely abolished by tryptic digestion of the RYR2 luminal face [39,45], a parallel luminal process likely occurs.

By studying divalent-metal cation selectivity of the RYR2 luminal face in combination with bioinformatics, we recently positioned the luminal Ca^{2+} site with the EF-hand structure to the genuine luminal region (the first luminal loop connecting the first and second transmembrane segments), which is indeed exposed to the luminal environment [39]. In this study, we provide further strong evidence in support of the luminal Ca^{2+} site on the RYR2 channel using a trivalent cation, Eu^{3+} . Because trivalent cations possess high binding affinities for Ca^{2+} sites and do not permeate Ca^{2+} channel pores, Eu^{3+} is an excellent experimental tool for directly manipulating only the luminal component of RYR2 regulation by luminal Ca^{2+} . At the single-channel level, we found that luminal Eu^{3+} modified the caffeine-activated RYR2 channel when bathed with luminal Ca^{2+} . No appreciable effect was revealed for luminal Ba^{2+} (mimicking the absence of luminal Ca^{2+}). Importantly, distinct RYR2 gating modes acquired in the presence of luminal Ca^{2+} or Ba^{2+} were resistant to luminal Eu^{3+} . Under our experimental conditions, essential determinants of the Ca^{2+} feedthrough mechanism (such as the Ca^{2+} current and RYR2 sensitivity to cytosolic Ca^{2+}) were not affected. This implies that the RYR2 cytosolic face was not likely involved in the observed changes because luminal Ca^{2+} emanating from the open channel pore led to a continual buildup of the Ca^{2+} concentration on the cytosolic side during channel opening [46]. Taken together, our results indicate that two spatially distinct Ca^{2+} sites, accessible from the RYR2 luminal side even when the channel is closed, likely mediate true luminal regulation by independently controlling RYR2 sensitivity to caffeine and gating behavior.

2. MATERIAL AND METHODS

2.1. Preparation of membrane vesicles

All procedures with male Wistar rats were approved by the State veterinary and food administration of the Slovak Republic (Ro-2721/17-221). Sarcoplasmic reticulum (SR) microsomes enriched in RYR2 channels were isolated from the ventricles of adult rat hearts as previously described [41]. Because the SR microsomes yielded a detectable amount of CSQ2 [43], we removed it during the isolation by the inclusion of 15 mM CaCl_2 in the isolation solutions, except the final resuspension buffer.

2.2. Drugs and chemicals

Phospholipids were obtained from Avanti Polar Lipids, Inc. (Alabaster, AL). All other chemicals were from Sigma-Aldrich (St. Louis, MO), if not stated otherwise.

2.3. Single - channel recordings

Activity of RYR2 channels incorporated into planar lipid membranes (BLMs) were recorded under voltage-clamp conditions. The BLMs of a 3:1 mixture of 1,2-dioleoyl-*sn*-glycero-3-phosphoethanolamine (DOPE) and 1,2-dioleoyl-*sn*-glycero-3-[phospho-L-serine] (DOPS) were painted on 50–70 μm diameter circular apertures in the wall of a polystyrene cup. The *cis* chamber (corresponding to cytosol) was filled with 1 ml of 100 mM HEPES, ~ 48 mM Tris, 50 mM KCl (pH = 7.35), and the *trans* chamber (corresponding to lumen) was filled with 1 ml of 8 mM $\text{Ca}(\text{OH})_2$ or $\text{Ba}(\text{OH})_2$, 50 mM KCl, ~ 22 mM HEPES (pH = 7.35). The current (always in the lumen-to-cytosol direction) was carried by Ca^{2+} or Ba^{2+} cations. Cytosolic caffeine or in some cases cytosolic Ca^{2+} was used to gradually activate RYR2 channels up to the maximal level. In the *cis* solution, the free cytosolic Ca^{2+} concentration ($[\text{Ca}^{2+}]_c$) was obtained by including 1 mM ethylene glycol-bis(2-aminoethylether)-

N,N,N',N'- tetraacetic acid (EGTA) and appropriate concentration of CaCl_2 as calculated by WinMaxc32 version 2.50 (<http://www.stanford.edu/~cpatton/maxc.html>). When caffeine was used as a channel activator, $[\text{Ca}^{2+}]_C$ was adjusted to 100 nM. The *trans* chamber was connected to the head-stage input of an Axopatch 200B amplifier (Molecular Devices, Sunnyvale, CA) and the *cis* chamber was held at ground. The holding potential was 0 mV in all experiments, except when studying RYR2 conductance in which a range of holding potentials from -30 mV to +30 mV was applied. In addition, to transiently relieve permanent total blockage of the RYR2 pore by luminal Eu^{3+} , a negative holding potential (-30 mV, *trans* versus *cis*) was applied for 30 s to repulse Eu^{3+} out of the pore. Electrical signals were filtered through an Axopatch 200B low-pass Bessel filter at 1 kHz, digitized at 4 kHz with an A/D-D/A converter (Digidata 1550A, Molecular Devices, Sunnyvale, CA).

2.4. Single - channel analysis

Data acquisition and analysis were performed with a commercially available software package (pCLAMP 10.5, Molecular Devices, Sunnyvale, CA). The open probability (P_O) was calculated from continuous records of > 2 min in duration using the 50%-amplitude threshold method. For each dataset, dependence of P_O on caffeine concentration was globally fitted by the Hill function with no shared parameters,

$$P_O = P_O^{\min} + (P_O^{\max} - P_O^{\min}) \frac{[\text{caffeine}]^{n_H}}{[\text{caffeine}]^{n_H} + EC_{50}^{n_H}}, \quad (1)$$

where the P_O^{\min} was fixed to the P_O value in the absence of caffeine. Other fitted parameters, such as the maximal achievable P_O induced by caffeine (P_O^{\max}), the half-activating caffeine concentration (EC_{50}) and the Hill coefficient (n_H), were free. For each dataset, the P_O^{\min} , P_O^{\max} and EC_{50} values were further averaged. For gating analysis, the records were divided into 30-s intervals. On these intervals, the frequency of opening (F) was calculated as a number of openings per 1 s and the P_O was determined, as usual. The average open (T_O) and closed times (T_C) were calculated as a standard arithmetic average. The resulting values of F , T_O and T_C for each dataset were further averaged on defined P_O -intervals and statistically compared. The P_O -dependence of F was fitted by the polynomial function of degree two and the maximal F (F^{\max}) was determined. Current amplitude calculations were made by measuring the difference between means of two Gaussian curves fitted to all-points amplitude histograms generated from continuous records of 30 s in duration. The results are reported as average \pm SEM. The values of F^{\max} are reported with the standard error calculated from the standard errors of the fitted parameters. Statistical comparisons ($P < 0.05$) of differences were made by the one-way ANOVA with the Tukey's post hoc test.

3. RESULTS

RYR2 channels stripped of CSQ2 were incorporated into the BLMs and recorded under asymmetric conditions when either 8 mM luminal Ca^{2+} ($[\text{Ca}^{2+}]_L$) or 8 mM luminal Ba^{2+} ($[\text{Ba}^{2+}]_L$) was present and used as a sole charge carrier. Luminal Ba^{2+} mimicked the situation when no Ca^{2+} was present on the RYR2 luminal face. At 0 mV, the flow of Ca^{2+} or Ba^{2+} in the lumen-to-cytosol direction was favored. It has been proposed that the effects of luminal Ca^{2+} must transpire through the modulation of RYR2 responsiveness to cytosolic modulators [47], in order to explain the propagation of arrhythmogenic Ca^{2+} waves in cardiac muscle cells [48]. Therefore, we activated RYR2 channels by cytosolic caffeine or in some cases by

cytosolic Ca^{2+} . We acquired dose-response curves for each RYR2 channel and examined the effects of tested luminal conditions over the whole range of channel activity. For experiments with caffeine, the free cytosolic Ca^{2+} concentration ($[\text{Ca}^{2+}]_c$) was adjusted to 100 nM, which left the cytosolic Ca^{2+} site mostly vacant. For the same channel, the response to caffeine or cytosolic Ca^{2+} was first recorded under control conditions (0 mM luminal Eu^{3+} , $[\text{Eu}^{3+}]_L$) and consequently after luminal Eu^{3+} was added, following cytosolic agonist washout.

3.1. Effects of luminal Eu^{3+} on the conducting properties of the RYR2 channel

Trivalent cations have high affinities for Ca^{2+} sites in proteins [49] and cannot cross biological membranes because they strongly bind inside the conductive pore of Ca^{2+} channels, causing permanent physical occlusion [50-53]. Thus, we employed luminal Eu^{3+} to directly interfere with the true luminal mechanism only (Schematic 1). To explore this luminal action of Eu^{3+} , in an unbiased manner, it was necessary to verify the non-permeant nature and lack of Eu^{3+} impact on Ca^{2+} and Ba^{2+} currents before Eu^{3+} enters the channel pore. We sequentially applied various $[\text{Eu}^{3+}]_L$ to caffeine-activated RYR2 channels to produce a concentration gradient through the BLM that was high enough to drive Eu^{3+} to the channel pore and induce its permanent total blockage, and concurrently, define the experimental range of $[\text{Eu}^{3+}]_L$ available for functional testing. Regarding the Ca^{2+} current, 5 mM $[\text{Eu}^{3+}]_L$ abolished the channel activity (Fig. 1A). Because Ba^{2+} has a lower binding affinity in the RYR2 pore than Ca^{2+} [54,55], we expected its lower potency to competitively antagonize the blocking action of Eu^{3+} . Regarding the Ba^{2+} current, indeed, 4 mM $[\text{Eu}^{3+}]_L$ induced a permanent pore occlusion (Fig. 1B, top trace). To clearly show that Eu^{3+} blocked the channel by substituting for permeant Ca^{2+} or Ba^{2+} inside the channel pore, we applied a negative potential to repulse Eu^{3+} from the pore. In only one Ba^{2+} experiment, we successfully restored RYR2 activity by applying -30 mV for 30 s (Fig. 1B, bottom trace). More negative potentials broke the BLMs in each case. To exclude any potential impact of luminal Eu^{3+} on the RYR2 conducting properties before permanent total blockage occurred, current-voltage relationships of the caffeine-activated RYR2 channel were measured in the presence of 0–4 mM $[\text{Eu}^{3+}]_L$ when Ca^{2+} was the charge-carrying ion, or 0–3 mM $[\text{Eu}^{3+}]_L$ when Ba^{2+} was the permeating ion. Luminal Eu^{3+} caused no significant changes in Ca^{2+} and Ba^{2+} conductance, slightly varying between 123.7 ± 5.8 pS and 129.5 ± 4.8 pS for Ca^{2+} and between 164 ± 10 pS and 183 ± 14 pS for Ba^{2+} (Fig. 1C). Similarly, luminal Eu^{3+} did not alter the Ca^{2+} and Ba^{2+} currents at 0 mV, which ranged from 1.741 ± 0.099 pA to 2.25 ± 0.24 pA and from 2.43 ± 0.38 pA to 2.84 ± 0.31 pA, respectively (Fig. 1C). Finally, we searched for subconductance openings to current levels less than the maximum level as a manifestation of a transient partial blockage of the RYR2 pore. All-points amplitude histograms are shown for the Ca^{2+} and Ba^{2+} current traces (Supplemental Figs. S1 A and B, respectively) in the control and after adding the lowest and the highest $[\text{Eu}^{3+}]_L$ tested. In all cases, the distributions were well fitted by the sum of two Gaussian functions. This implies that luminal Eu^{3+} did not induce any subconductance levels because only two peaks corresponding to the main closed and open channel states were identified in histograms. Overall, all observed Eu^{3+} characteristics are consistent with the action of total-pore-blocking agents [56]. Luminal Eu^{3+} does indeed physically block the RYR2 pore, and before permanent lodging within the channel conductance pathway, it does not interfere with the RYR2 conducting properties. Furthermore, our results clearly indicate that $[\text{Eu}^{3+}]_L < 5$ mM in mixture with 8 mM $[\text{Ca}^{2+}]_L$ or $[\text{Eu}^{3+}]_L < 4$ mM in mixture with 8 mM $[\text{Ba}^{2+}]_L$ could be safely used to gain a further insight into RYR2 regulation by luminal Ca^{2+} .

3.2. Regulation of the RYR2 channel by luminal Eu^{3+} in the presence of luminal Ca^{2+}

Several reports have shown that caffeine-dependent RYR2 activation is significantly enhanced by both cytosolic [15,41,57] and luminal Ca^{2+} [39,41,42,58,59]. Our aim in this study was to investigate only luminal regulation of RYR2 responsiveness to caffeine; therefore, experiments were carried out at a non-activating $[\text{Ca}^{2+}]_C$ of 100 nM and with luminal Ca^{2+} present. Importantly, the Ca^{2+} current was not affected by the tested $[\text{Eu}^{3+}]_L$; thus, Ca^{2+} emanating from the RYR2 pore did not alter occupancy of the cytosolic Ca^{2+} site. Fig. 2A (top four traces) shows representative current traces of the RYR2 channel under the control condition (8 mM $[\text{Ca}^{2+}]_L$ + 0 mM $[\text{Eu}^{3+}]_L$), recorded at caffeine concentrations spanning the whole activation range (0–10 mM) to clearly illustrate the RYR2 behavior at a low, middle, and high P_O . Fig. 2A (bottom four traces) displays single-channel recordings obtained in the presence of 4 mM $[\text{Eu}^{3+}]_L$, the highest functional concentration tested. Under the control condition and also in the presence of luminal Eu^{3+} , short, fully resolved channel events were observed in the absence of caffeine. Elevation of the caffeine concentration significantly increased P_O to the maximal level when long open events were interrupted by brief closings. The effects of luminal Eu^{3+} on the dose-response to caffeine are illustrated in Fig. 2B (left). The solid lines show the best fits by the Hill equation (Eq. 1). Dependence of the fitted EC_{50} and P_O^{\max} values on $[\text{Eu}^{3+}]_L$ is displayed in Fig. 2B (right) and Supplemental Fig. S2 A (right), respectively. Elevation of $[\text{Eu}^{3+}]_L$ from 0 mM to 4 mM led to a significant increase in EC_{50} from 2.04 ± 0.23 mM to 5.60 ± 0.52 mM. Of note, luminal Eu^{3+} did not modulate RYR2 activity in the absence of caffeine, P_O^{\min} , or P_O^{\max} (Supplemental Fig. S2 A). These parameters changed only negligibly, ranging from 0.0041 ± 0.0016 to 0.0089 ± 0.0043 for P_O^{\min} and from 0.9759 ± 0.0067 to 0.996 ± 0.018 for P_O^{\max} . A growing consensus exists regarding the prolongation pattern in RYR2 gating parameters, the average open (T_O) and closed times (T_C), caused by luminal Ca^{2+} when caffeine or ATP are used for channel activation [26,39,43,44]. It was therefore of interest to assess how luminal Eu^{3+} impacts this typical RYR2 gating behavior. Fig. 3A shows representative RYR2 recordings in the presence of 0, 2 and 4 mM $[\text{Eu}^{3+}]_L$ when the channels reached P_O of ~ 0.5 . We considered this activity as the most predictive since the RYR2 channel opened and closed often enough to capture existing alterations in the gating pattern [39,41]. Notably, luminal Eu^{3+} did not appreciably affect the number of channel events. At the quantitative level, we determined T_O , T_C and the opening frequency (F) over the whole range of RYR2 activity increased by the addition of caffeine. The F data are summarized in Fig. 3B and the T_O and T_C data are presented in Supplemental Fig. S3 A (left and right, respectively). In our analysis, we focused on F because the values of T_O and T_C are simply encapsulated in this parameter (the reciprocal of the summation of T_O and T_C). Increasing $[\text{Eu}^{3+}]_L$ from 0 mM to 4 mM had no significant effect on the bell-shaped P_O -dependence of F (Fig. 3B, left). The solid lines are the best fits by the polynomial function of degree two, and the maximal value of F (F^{\max}) for 0–4 mM $[\text{Eu}^{3+}]_L$ was derived from the corresponding fit. No significant $[\text{Eu}^{3+}]_L$ -dependence was noted (Fig. 3B, right). The F^{\max} values achieved at $P_O \sim 0.5$ were similar, oscillating between $9.6 \pm 1.0 \text{ s}^{-1}$ and $10.6 \pm 1.1 \text{ s}^{-1}$. Similarly, no changes were observed in the P_O -dependencies of T_O and T_C (Supplemental Fig. S3 A, left and right, respectively). For all tested $[\text{Eu}^{3+}]_L$, T_O increased and T_C decreased with increasing P_O in a similar manner. The values of T_O and T_C at a given P_O -interval were independent of $[\text{Eu}^{3+}]_L$. Notably, we preferred to plot the gating parameters against P_O instead of the caffeine concentration because a tight relationship exists between channel gating and P_O , resulting in a smaller data dispersion (Supplemental Fig. S4). Moreover, P_O - and caffeine-dependencies exhibit similar shapes;

biphasic for F data with the same F^{\max} values (Supplemental Fig. S4 A), monotonically increasing for T_O data and decreasing for T_C data (Supplemental Fig. S4 B). Taken together, the EC_{50} results suggest that luminal Eu^{3+} may interact with the RYR2 channel on its luminal face by displacing Ca^{2+} from its luminal binding site, thereby causing changes in RYR2 responsiveness to caffeine. We tested this possibility by investigating the effects of 4 mM $[\text{Eu}^{3+}]_L$ on RYR2 sensitivity to cytosolic Ca^{2+} . Such Eu^{3+} action, likely inhibitory, could be also fully or partially responsible for the observed stepwise positive shift in the EC_{50} for caffeine. Fig. 4 (left) shows pooled results summarizing P_O values of the RYR2 channel after gradual activation by cytosolic Ca^{2+} up to the maximal level, in the presence or absence of luminal Eu^{3+} . The solid lines are the best fits by the Hill equation (Eq. 1). The fitted EC_{50} values for cytosolic Ca^{2+} (Fig. 4, right) and P_O^{\max} , as well as the calculated P_O^{\min} values are plotted against $[\text{Eu}^{3+}]_L$ (Supplemental Fig. S5). Under the control condition (0 mM $[\text{Eu}^{3+}]_L$), the EC_{50} was 252.1 ± 6.8 nM, the P_O^{\max} was 0.968 ± 0.015 and the P_O^{\min} was 0.0096 ± 0.0038 . None of these parameters were significantly changed by 4 mM $[\text{Eu}^{3+}]_L$, with the EC_{50} of 270 ± 12 nM, the P_O^{\max} of 0.928 ± 0.040 and the P_O^{\min} of 0.0141 ± 0.0056 . The results indicate that under our experimental conditions, the RYR2 cytosolic face does not likely mediate the observed impairment in caffeine-dependent RYR2 activation.

3.3. Regulation of the RYR2 channel by luminal Eu^{3+} in the presence of luminal Ba^{2+}

Previous evidence suggested that replacing luminal Ca^{2+} with alkaline earth metal cations such as Sr^{2+} , Mg^{2+} , or Ba^{2+} on the luminal face of the CSQ2-stripped RYR2 channel decreased RYR2 sensitivity to caffeine and significantly increased F [39,42]. Therefore, the lack of an appreciable impact of luminal Eu^{3+} on RYR2 gating was unexpected. This observation, however, could be rationalized if luminal Eu^{3+} exhibits a potency similar to luminal Ca^{2+} in decreasing F by prolonging T_O and T_C , albeit with a substantially reduced potency to sensitize the RYR2 channel to caffeine. We tested this idea using luminal Ba^{2+} . Fig. 5 shows a comparison of RYR2 function under the control condition and after luminal Eu^{3+} was added. Fig. 5A shows RYR2 recordings in the absence (top four traces) and presence of 3 mM $[\text{Eu}^{3+}]_L$, when cytosolic caffeine (0–14 mM) was used to stepwisely activate the channel up to the maximal level (bottom four traces). In Fig. 5B (left), caffeine-dependent RYR2 activation is displayed for 0–3 mM $[\text{Eu}^{3+}]_L$. The solid lines represent Hill equation fits (Eq. 1) and the fitted values of EC_{50} for caffeine (Fig. 5B, right), and P_O^{\max} (Supplemental Fig. S2 B, right) and the calculated values of P_O^{\min} (Supplemental Fig. S2 B, left) were plotted against $[\text{Eu}^{3+}]_L$ and compared. In contrast to luminal Ca^{2+} , no noticeable effect on EC_{50} was revealed, although, a trend toward reduction was observed (7.30 ± 0.51 mM at 0 mM $[\text{Eu}^{3+}]_L$ vs. 6.56 ± 0.62 mM at 3 mM $[\text{Eu}^{3+}]_L$). This behavior could not be further tested because of permanent total blockage of the RYR2 pore at $[\text{Eu}^{3+}]_L > 3$ mM (Fig. 1B). The P_O^{\min} and P_O^{\max} changed only negligibly and ranged from 0.00038 ± 0.00026 to 0.0044 ± 0.0015 and from 0.980 ± 0.026 to 0.999 ± 0.022 , respectively. Considering that we previously reported a strong ability of Ca^{2+} to displace Ba^{2+} , when added on the RYR2 luminal face [39], we can assume that 3 mM $[\text{Eu}^{3+}]_L$ is sufficient to compete with luminal Ba^{2+} . Thus, the functional effects of luminal Eu^{3+} on RYR2 activity could be manifested. Based on these data, it is evident that luminal Eu^{3+} and Ba^{2+} share similar potencies in modulating RYR2 activity in the presence of caffeine.

As we were particularly interested in whether luminal Eu^{3+} can affect RYR2 gating similarly to luminal Ca^{2+} , we calculated T_O , T_C , and F for all tested $[\text{Eu}^{3+}]_L$ and plotted these gating parameters as a function of P_O . Fig. 6A shows sample RYR2 recordings at 0, 1, and

3 mM $[\text{Eu}^{3+}]_{\text{L}}$ in the presence of 8 mM $[\text{Ba}^{2+}]_{\text{L}}$. At first glance, luminal Eu^{3+} clearly failed to produce any significant effect on RYR2 gating when caffeine activated the channel to $P_{\text{O}} \sim 0.5$. The durations of channel openings and closings were similar and not prolonged by luminal Eu^{3+} . A summary of the T_{O} and T_{C} data is displayed in Supplemental Fig. S3 B, and the F data are shown in Fig. 6B. For each tested $[\text{Eu}^{3+}]_{\text{L}}$, F showed a bell-shaped dependence on P_{O} fitted by the polynomial function of degree two (Fig. 6B, left, solid lines). The F^{max} values did not depend on $[\text{Eu}^{3+}]_{\text{L}}$ and fluctuated from $40.6 \pm 4.7 \text{ s}^{-1}$ to $43.8 \pm 4.4 \text{ s}^{-1}$ (Fig. 6B, right). In the absence of luminal Eu^{3+} , RYR2 P_{O} increased due to both an increase in T_{O} and a decrease in T_{C} (Supplemental Fig. S3 B). The overall shape of the P_{O} -dependencies of T_{O} and T_{C} remained unchanged when luminal Eu^{3+} was added. In addition, the T_{O} and T_{C} values were independent of $[\text{Eu}^{3+}]_{\text{L}}$ at all P_{O} -intervals. These results highlight the complexity of RYR2 regulation by luminal Ca^{2+} and indicate that gating behavior and responsiveness to caffeine could be governed by two distinct processes.

4. DISCUSSION

Chen et al. [8] and Jones et al. [40] attempted to manipulate the true luminal mechanism of RYR2 activation by luminal Ca^{2+} via side-directed mutagenesis. Testing the single-channel properties of various RYR2 mutants, they identified a putative E4872-containing Ca^{2+} pocket on the cytosolic face of the channel gate that could bind luminal Ca^{2+} . Notably, Jones et al. [40] further hypothesized that this novel Ca^{2+} pocket, contrary to the constitutively present cytosolic Ca^{2+} site, is formed only transiently when the RYR2 channel is in the open conformation. In this study, we probed the true luminal mechanism employing a completely different approach, based on the non-permeant properties of trivalent cations with respect to Ca^{2+} channels. In addition, trivalent cations strongly interfere with Ca^{2+} activity in vivo, substituting for Ca^{2+} in various Ca^{2+} sites [60, 61]. Therefore, trivalent cations can displace Ca^{2+} from its binding sites and directly operate only on one side of the membrane (the side to which they are added). Our data indicate that the true luminal component of luminal Ca^{2+} -mediated RYR2 regulation most likely involves two distinct Ca^{2+} sites that independently control channel responsiveness to cytosolic caffeine and gating behavior, possibly functioning parallel to a recently identified luminal Ca^{2+} sensor in the cytosolic region of the RYR2 gate.

4.1. Eu^{3+} binding properties of the RYR2 luminal face

Fig. 7 schematically recapitulates the central finding of this study, correlating luminal Ca^{2+} and Ba^{2+} data. In the presence of luminal Ca^{2+} , the RYR2 response to caffeine was graded and controlled by $[\text{Eu}^{3+}]_{\text{L}}$. Specifically, 4 mM $[\text{Eu}^{3+}]_{\text{L}}$ almost completely antagonized the potentiating effects of 8 mM $[\text{Ca}^{2+}]_{\text{L}}$, as the dose-response curve for caffeine was substantially shifted to the right, close to that plotted for luminal Ba^{2+} . Moreover, when luminal Ba^{2+} was substituted for Ca^{2+} , 3 mM $[\text{Eu}^{3+}]_{\text{L}}$ caused only a negligible shift in the opposite direction, to the left (Fig. 7A, left). Although a higher $[\text{Eu}^{3+}]_{\text{L}}$ could not be tested because permanent total blockage of the RYR2 pore occurred, our functional data already provide sufficient information. To correctly interpret our results, we have to consider that the RYR2 channel is a huge allosteric protein; therefore, luminally added Eu^{3+} could still indirectly manipulate its cytosolic face. However, there are several arguments against this model. Firstly, we found that under our experimental conditions, Ca^{2+} permeation (Fig. 1C) was not affected over the tested range of $[\text{Eu}^{3+}]_{\text{L}} < 5 \text{ mM}$. This implies that the Ca^{2+} current led to the buildup of a constant $[\text{Ca}^{2+}]_{\text{C}}$ near the cytosolic Ca^{2+} site during each opening event [46]. Secondly, luminal Ca^{2+} accumulation on the cytosolic face depends only on amplitude of the Ca^{2+} current. This process is not controlled by the channel activity because the Ca^{2+}

gradient forming around the open RYR2 channel dissipates immediately when the channel closes [62]. Thus, reduced RYR2 activity due to luminal Eu^{3+} would not decrease occupancy of the cytosolic Ca^{2+} site, which would otherwise require a higher caffeine concentration to activate the channel. Thirdly, since cytosolic Ca^{2+} sensitizes the RYR2 channel to caffeine, and therefore, the observed shift in the dose-response to caffeine could result from impaired cytosolic Ca^{2+} -dependent RYR2 activation, we revealed that this is clearly not the case. We evidenced that luminal Eu^{3+} did not alter the RYR2 response to Ca^{2+} directly added to the cytosolic face (Fig. 4). Finally, Porta et al. [59] reported that the Ca^{2+} feedthrough mechanism is manifested only when the Ca^{2+} current is large enough (> 3 pA). Because under our experimental conditions of 0 mV and 8 mM $[\text{Ca}^{2+}]_{\text{L}}$, the Ca^{2+} current was < 3 pA (Fig. 1C) and was not increased by luminal Eu^{3+} , it is reasonable to assume that the cytosolic face shows minor participation, if it participates at all. Considering the aforementioned arguments as well as the combined Ca^{2+} and Ba^{2+} data, we may conclude that luminal Eu^{3+} likely competed with luminal Ca^{2+} or Ba^{2+} on the RYR2 luminal face. This competition resulted in substantial inhibition of the caffeine-activated RYR2 channel in the presence of luminal Ca^{2+} , and slight, but not significant, RYR2 activation in the presence of luminal Ba^{2+} . These results are consistent with recently published data documenting a weak activation potency of Eu^{3+} at the vacant cytosolic Ca^{2+} site of the skeletal RYR1 isoform [53]. Two interesting points emerge from our data. Firstly, a lumenally located Ca^{2+} site controlling the RYR2 response to caffeine indeed exists and is freely accessible for luminal Eu^{3+} . Thus, it might be located in the genuine luminal region of the channel, presumably on the luminal loops connecting the transmembrane helices (Fig. 7A, right). Secondly, the RYR2 luminal Ca^{2+} site possesses preferential selectivity towards Eu^{3+} over alkaline earth metal cations, as Eu^{3+} appeared to be a significantly more potent antagonist of Ca^{2+} than Sr^{2+} , Mg^{2+} , or Ba^{2+} in competition assays (Fig. 8A). Moreover, we previously evidenced a strong discrimination among alkaline earth metal cations on the RYR2 luminal face [39]. These attributes are typical for well-structured Ca^{2+} sites identified so far in proteins [60,61]; thus, it is highly unlikely that the luminal Ca^{2+} site on the RYR2 channel is only a simple cluster of negatively charged amino acid residues.

It is well documented that luminal Ca^{2+} has a marked effect on RYR2 gating [8,26,39,41-44]. In the presence of luminal Ca^{2+} (> 1 mM), RYR2 channels activated by caffeine or ATP exhibit substantially long open and closed events (Figs. 2A and 3A). This specific behavior has been attributed to the true luminal mechanism because luminal Ca^{2+} would not be expected to prolong T_{C} , other than by interacting with the luminal face of the closed RYR2 channel [17,41]. Furthermore, when comparing similar P_{O} values, caffeine with luminal Ca^{2+} opened and closed the RYR2 channel less frequently than did caffeine with cytosolic Ca^{2+} . Finally, such prolongation in T_{O} and T_{C} was evidenced only for luminal Ca^{2+} when compared with other permeant alkaline earth metal cations [39,42], which were, however, able to compete with luminal Ca^{2+} and substantially increase F by shortening T_{O} and T_{C} [39]. Surprisingly, our current results show that luminal Eu^{3+} did not affect RYR2 gating specific for luminal Ca^{2+} or Ba^{2+} , although a mutual competition took place, considering the caffeine EC_{50} values. In both cases, the channel opened and closed similarly, regardless of the presence of luminal Eu^{3+} (Figs. 7B, left and 8B). If RYR2 gating was a target of luminal Eu^{3+} , then it should be manifested by either an increase in F^{max} when competing with luminal Ca^{2+} or a decrease in F^{max} when competing with luminal Ba^{2+} . However, this was clearly not the case. The reason for the observed phenomenon probably lies in the existence of an additional Ca^{2+} site contributing to the true luminal mechanism that apparently does not interact with luminal Eu^{3+} because of its specific location (Figs. 7A and B, right).

4.2. Implications for location of Ca^{2+} sites involved in true luminal regulation of the RYR2 channel

Although the exact nature of proposed RYR2 Ca^{2+} sites involved in the true luminal mechanism is uncertain, we previously identified an EF-hand region within the first luminal loop of mammalian RYR2 channels using the EF-hand motif signature [39], which is the most straightforward way to highlight EF-hand-positive regions even in the primary sequence of proteins [63,64]. The 3D structure of this luminal loop has not been resolved yet to validate our hypothesis [14]. The main obstacle is its substantial conformational flexibility, which is typical for protein loops in general. Therefore, it is difficult to solve its 3D structure by X-ray crystallography or to model it using standard homology modeling [65,66]. Despite all this, the relevance of the luminal Ca^{2+} site on the RYR2 channel has received support from studies of stromal interaction molecule 1 (STIM1). STIM1 is a luminal Ca^{2+} sensor that plays an essential role in store-operated Ca^{2+} entry [67,68]. Particularly, STIM1 is responsible for activating the Ca^{2+} release-activated Ca^{2+} (CRAC) channel by sensing changes in $[\text{Ca}^{2+}]_{\text{L}}$ via its luminal EF-hand site. Consistent with our results, STIM1 luminal Ca^{2+} site possesses a higher binding affinity for trivalent cations, such as Tb^{3+} , than for Ca^{2+} ($K_{\text{D}} = 170 \pm 6 \mu\text{M}$ vs. $512 \pm 15 \mu\text{M}$, respectively) [69]. Further evidence of the importance of the first RYR2 luminal loop in Ca^{2+} accommodation comes from the work by Chen et al. [70] demonstrating Ca^{2+} binding to the short RYR1 fragment encompassing the first luminal loop. This finding can be extrapolated to the RYR2 channel because of high sequence identity between the RYR1 and RYR2 isoforms, especially in the membrane domain [71]. Thus, the first luminal loop of the RYR2 channel appears to be most likely involved in the true luminal mechanism of channel regulation by luminal Ca^{2+} .

The lack of significant competitive effects of luminal Eu^{3+} on RYR2 gating might be indicative of the presence of an additional Ca^{2+} site that apparently does not interact with luminal Eu^{3+} . It could reasonably be expected to reside in the RYR2 pore, where the appearance of Eu^{3+} is restricted. This region, lined with negatively charged residues accommodating various cations, is essential for transport of mono- and divalent cations and is occupied even when the RYR2 channel is closed [8]; thus, the main principle of the true luminal mechanism would not be violated. Even though detailed information on the physical structures involved in cation permeation via the RYR2 pore is still not available, four distinct Ca^{2+} binding regions, highlighted by computational simulations utilizing 3D structural data [72], could be considered to govern RYR2 gating. Two major Ca^{2+} sites were identified in the luminal vestibule near D4832 and in the adjacent selectivity filter, including G4823. Two minor Ca^{2+} sites reside in the luminal and cytosolic regions of the RYR2 gate, situated around Q4862 and E4872, respectively (Fig. 7B, right). Interestingly, the last interaction site in the lumen-to-cytosol direction is identical to that highlighted by Chen et al. [8] and Jones et al. [40] and formed by E4872, D4875, E4878, and Q4879. Because this site is accessible for luminal Ca^{2+} only when the RYR2 channel is open, we did not consider it. According to computational models, trivalent cations enter Ca^{2+} channel pores and permanently bind within the selectivity filter [54,55,73] causing a total pore blockage. At this position, the effects on RYR2 gating could be still present for permeant cations, but could not be manifested for luminal Eu^{3+} . This idea is further supported by strong evidence for significant role of selectivity filter dynamics in the gating behavior of K^{+} channels [74,75]. Two remaining Ca^{2+} sites (one in the luminal vestibule, not attractive for luminal Eu^{3+} because of a low binding affinity, and the other in the luminal region of the RYR2 gate, not accessible for luminal Eu^{3+}) could also participate in gating regulation. Particularly, a cluster of negatively charged residues in the luminal mouth of the channel gate was indeed highlighted as an important structural element potentially involved in the true luminal mechanism [40].

4.3. Pathophysiological implications for CPVT

CPVT is a highly malignant arrhythmogenic disorder occurring under stress conditions [8], predominantly caused by gain-of-function mutations in the gene encoding the human RYR2 channel [76,77]. Abnormal luminal Ca^{2+} regulation of RYR2 mutants can lead to the initiation and propagation of arrhythmogenic Ca^{2+} waves. Far over 150 RYR2 mutations have been identified that appear to cause CPVT (reviewed in [78]). However, only 2 of them are situated in the first luminal loop (A4556T [79] and S4565R [80]), not in the putative EF-hand region. This implies that the binding affinity of the luminal Ca^{2+} site might not be impaired; rather, interactions between Ca^{2+} binding on the RYR2 luminal face and allosteric CPVT mutations that influence the channel response to luminal Ca^{2+} (even though they are far away from the luminal Ca^{2+} site) might be targeted in CPVT syndrome. Thus, it seems reasonable to assume that RYR2 mutants would be still able to interact with luminal Eu^{3+} . Since CPVT mutations oversensitize the RYR2 channel to luminal Ca^{2+} , a similar situation could also be expected for luminal Eu^{3+} . For some RYR2 mutants, enhanced caffeine sensitivity has been demonstrated [81,82]; therefore, luminal Eu^{3+} could be expected to fully or partially correct the impaired channel function induced by CPVT mutations. Whether this scenario appears to be likely is yet to be determined.

5. CONCLUSIONS

The results obtained here suggest that the RYR2 channel possess two spatially distinct Ca^{2+} sites most likely conferring the true luminal mechanism of the complex RYR2 regulation by luminal Ca^{2+} . One site governing channel responsiveness to caffeine at low $[\text{Ca}^{2+}]_c$ is presumably located within the first luminal loop, and the RYR2 gating behavior is under control of the Ca^{2+} site, positioned within the channel pore. We describe a parallel luminal regulatory pathway to that identified by Chen et al. [8] and Jones et al. [40]. Their hypothesis highlights the role of the E4872-containing Ca^{2+} pocket that is transiently formed and accessible only when the channel opens. In our study, the function of this site was not likely manifested because of its delicate conformation achieved only when the synergetic action of more cytosolic RYR2 activators was present (ATP, caffeine, cytosolic Ca^{2+}). In accordance with this concept, the E4872A mutation led to a significant decrease in RYR2 sensitivity to both luminal and cytosolic Ca^{2+} [8]; however, luminal Eu^{3+} selectively manipulated only the responsiveness to luminal Ca^{2+} . This finding implies that the luminal Ca^{2+} sensor of the RYR2 channel could consist of more Ca^{2+} sites with distinct locations and functions, and their relative contributions are likely dependent on the functional state of the channel.

DECLARATION OF COMPETING INTEREST

The authors declare no competing financial interests.

ACKNOWLEDGEMENTS

We are grateful for the technical assistance with animal sacrifice provided by Lubica Malekova. Veronika Drevenakova and Monika Drozdova assisted with the early BLM experiments. This work was supported by the Slovak scientific grant agency (grants VEGA 2/0011/18 to J.G. and VEGA 2/0086/17 to M.G.) and EU Structural Fund ITMS 26230120009. The funder had no role in study design, data collection, analysis and interpretation, decision to publish, or preparation of the manuscript.

REFERENCES

- [1] A. Fabiato, Calcium-induced release of calcium from the cardiac sarcoplasmic reticulum, *Am. J. Physiol.* 245 (1983) C1-14.
- [2] H. Cheng, W.J. Lederer, M.B. Cannell, Calcium sparks: elementary events underlying excitation-contraction coupling in heart muscle, *Science* 262 (1993) 740-744.
- [3] L.F. Santana, H. Cheng, A.M. Gomez, M.B. Cannell, W.J. Lederer, Relation between the sarcolemmal Ca^{2+} current and Ca^{2+} sparks and local control theories for cardiac excitation-contraction coupling, *Circ. Res.* 78 (1996) 166-171.
- [4] S.O. Marx, S. Reiken, Y. Hisamatsu, T. Jayaraman, D. Burkhoff, N. Rosembli, A.R. Marks, PKA phosphorylation dissociates FKBP12.6 from the calcium release channel (ryanodine receptor): defective regulation in failing hearts, *Cell* 101 (2000) 365-376.
- [5] S. Reiken, M. Gaburjakova, J. Gaburjakova, K.L. He Kl, A. Prieto, E. Becker, G.H. Yi Gh, J. Wang, D. Burkhoff, A.R. Marks, Beta-adrenergic receptor blockers restore cardiac calcium release channel (ryanodine receptor) structure and function in heart failure, *Circulation* 104 (2001) 2843-2848.
- [6] S. Reiken, X.H. Wehrens, J.A. Vest, A. Barbone, S. Klotz, D. Mancini, D. Burkhoff, A.R. Marks, Beta-blockers restore calcium release channel function and improve cardiac muscle performance in human heart failure, *Circulation* 107 (2003) 2459-2466.
- [7] J. Shan, M.J. Betzenhauser, A. Kushnir, S. Reiken, A.C. Meli, A. Wronska, M. Dura, B.X. Chen, A.R. Marks, Role of chronic ryanodine receptor phosphorylation in heart failure and β -adrenergic receptor blockade in mice, *J. Clin. Invest.* 120 (2010) 4375-4387.
- [8] W. Chen, R. Wang, B. Chen, X. Zhong, H. Kong, Y. Bai, Q. Zhou, C. Xie, J. Zhang, A. Guo, X. Tian, P.P. Jones, M.L. O'Mara, Y. Liu, T. Mi, L. Zhang, J. Bolstad, L. Semeniuk, H. Cheng, J. Zhang, J. Chen, D.P. Tieleman, A.M. Gillis, H.J. Duff, M. Fill, L.S. Song, S.R. Chen, The ryanodine receptor store-sensing gate controls Ca^{2+} waves and Ca^{2+} -triggered arrhythmias, *Nat. Med.* 20 (2014) 184-192.
- [9] A. Fabiato, Time and calcium dependence of activation and inactivation of calcium-induced release of calcium from the sarcoplasmic reticulum of a skinned canine cardiac Purkinje cell, *J. Gen. Physiol.* 85 (1985) 247-289.
- [10] R.H. Ashley, A.J. Williams, Divalent cation activation and inhibition of single calcium release channels from sheep cardiac sarcoplasmic reticulum, *J. Gen. Physiol.* 95 (1990) 981-1005.
- [11] M.D. Stern, Theory of excitation-contraction coupling in cardiac muscle, *Biophys. J.* 63 (1992) 497-517.
- [12] M. Gaburjakova, J. Gaburjakova, Insight towards the identification of cytosolic Ca^{2+} -binding sites in ryanodine receptors from skeletal and cardiac muscle, *Acta Physiol.* 219 (2017) 757-767.
- [13] A. des Georges, O.B. Clarke, R. Zalk, Q. Yuan, K.J. Condon, R.A. Grassucci, W.A. Hendrickson, A.R. Marks, J. Frank, Structural basis for gating and activation of RyR1, *Cell* 167 (2016) 145-157.
- [14] W. Peng, H. Shen, J. Wu, W. Guo, X. Pan, R. Wang, S.R. Chen, N. Yan, Structural basis for the gating mechanism of the type 2 ryanodine receptor RyR2, *Science* 354 (2016) aah5324.
- [15] T. Murayama, H. Ogawa, N. Kurebayashi, S. Ohno, M. Horie, T. Sakurai, A tryptophan residue in the caffeine-binding site of the ryanodine receptor regulates Ca^{2+} sensitivity, *Commun. Biol.* 1 (2018) 98.
- [16] S. Györke, I. Györke, V. Lukyanenko, D. Terentyev, S. Viatchenko-Karpinski, T.F. Wiesner, Regulation of sarcoplasmic reticulum calcium release by luminal calcium in cardiac muscle, *Front. Biosci.* 7 (2002) d1454-1463.

- [17] D.R. Laver, Ca^{2+} stores regulate ryanodine receptor Ca^{2+} release channels via luminal and cytosolic Ca^{2+} sites, *Clin. Exp. Pharmacol. Physiol.* 34 (2007) 889-896.
- [18] S. Gyorke, D. Terentyev, Modulation of ryanodine receptor by luminal calcium and accessory proteins in health and cardiac disease, *Cardiovasc. Res.* 77 (2008) 245-255.
- [19] N.A. Beard, L. Wei, A.F. Dulhunty, Control of muscle ryanodine receptor calcium release channels by proteins in the sarcoplasmic reticulum lumen, *Clin. Exp. Pharmacol. Physiol.* 36 (2009) 340-345.
- [20] D. Jiang, R. Wang, B. Xiao, H. Kong, D.J. Hunt, P. Choi, L. Zhang, S.R. Chen, Enhanced store overload-induced Ca^{2+} release and channel sensitivity to luminal Ca^{2+} activation are common defects of RyR2 mutations linked to ventricular tachycardia and sudden death, *Circ. Res.* 97 (2005) 1173-1181.
- [21] D.E. Vatner, N. Sato, K. Kiuchi, R.P. Shannon, S.F. Vatner, Decrease in myocardial ryanodine receptors and altered excitation-contraction coupling early in the development of heart failure, *Circulation* 90 (1994) 1423-1430.
- [22] T. Yamamoto, M. Yano, M. Kohno, T. Hisaoka, K. Ono, T. Tanigawa, Y. Saiki, Y. Hisamatsu, T. Ohkusa, M. Matsuzaki, Abnormal Ca^{2+} release from cardiac sarcoplasmic reticulum in tachycardia-induced heart failure, *Cardiovasc. Res.* 44 (1999) 146-155.
- [23] T.R. Shannon, F. Wang, D.M. Bers, Regulation of cardiac sarcoplasmic reticulum Ca release by luminal $[\text{Ca}]$ and altered gating assessed with a mathematical model, *Biophys. J.* 89 (2005) 4096-4110.
- [24] I. Gyorke, S. Gyorke, Regulation of the cardiac ryanodine receptor channel by luminal Ca^{2+} involves luminal Ca^{2+} sensing sites, *Biophys. J.* 75 (1998) 2801-2810.
- [25] R. Sitsapesan, A.J. Williams, Regulation of the gating of the sheep cardiac sarcoplasmic reticulum Ca^{2+} -release channel by luminal Ca^{2+} , *J. Membr. Biol.* 137 (1994) 215-226.
- [26] L. Xu, G. Meissner, Regulation of cardiac muscle Ca^{2+} release channel by sarcoplasmic reticulum luminal Ca^{2+} , *Biophys. J.* 75 (1998) 2302-2312.
- [27] Y. Liu, M. Porta, J. Qin, J. Ramos, A. Nani, T.R. Shannon, M. Fill, Flux regulation of cardiac ryanodine receptor channels, *J. Gen. Physiol.* 135 (2010) 15-27.
- [28] D.R. Laver, B.N. Honen, Luminal Mg^{2+} , a key factor controlling RYR2-mediated Ca^{2+} release: cytoplasmic and luminal regulation modeled in a tetrameric channel, *J. Gen. Physiol.* 132 (2008) 429-446.
- [29] D.R. Laver, Luminal Ca^{2+} activation of cardiac ryanodine receptors by luminal and cytoplasmic domains, *Eur. Biophys. J.* 39 (2009) 19-26.
- [30] R.D. Mitchell, H.K.B. Simmerman, L.R. Jones, Ca^{2+} binding effects on protein conformation and protein interactions of canine cardiac calsequestrin, *J. Biol. Chem.* 263 (1988) 1376-1381.
- [31] B.T. Scott, H.K. Simmerman, J.H. Collins, B. Nadal-Ginard, L.R. Jones, Complete amino acid sequence of canine cardiac calsequestrin deduced by cDNA cloning, *J. Biol. Chem.* 263 (1988) 8958-8964.
- [32] N. Ikemoto, M. Ronjat, L.G. Meszaros, M. Koshita, Postulated role of calsequestrin in the regulation of calcium release from sarcoplasmic reticulum, *Biochemistry (Mosc.)* 28 (1989) 6764-6771.
- [33] I. Gyorke, N. Hester, L.R. Jones, S. Gyorke, The role of calsequestrin, triadin, and junctin in conferring cardiac ryanodine receptor responsiveness to luminal calcium, *Biophys. J.* 86 (2004) 2121-2128.
- [34] J. Qin, G. Valle, A. Nani, A. Nori, N. Rizzi, S.G. Priori, P. Volpe, M. Fill, Luminal Ca^{2+} regulation of single cardiac ryanodine receptors: insights provided by calsequestrin and its mutants, *J. Gen. Physiol.* 131 (2008) 325-334.

- [35] J. Qin, G. Valle, A. Nani, H. Chen, J. Ramos-Franco, A. Nori, P. Volpe, M. Fill, Ryanodine receptor luminal Ca^{2+} regulation: swapping calsequestrin and channel isoforms, *Biophys. J.* 97 (2009) 1961-1970.
- [36] A. Handhale, C.E. Ormonde, N.L. Thomas, C. Bialesford, A.J. Williams, F.A. Lai, S. Zissimopoulos, Calsequestrin interacts directly with the cardiac ryanodine receptor luminal domain, *J. Cell Sci.* 129 (2016) 3983-3988.
- [37] D. Terentyev, S. Viatchenko-Karpinski, I. Gyorke, P. Volpe, S.C. Williams, S. Gyorke, Calsequestrin determines the functional size and stability of cardiac intracellular calcium stores: Mechanism for hereditary arrhythmia, *Proc. Natl. Acad. Sci. U. S. A.* 100 (2003) 11759-11764.
- [38] M. Gaburjakova, N.C. Bal, J. Gaburjakova, M. Periasamy, Functional interaction between calsequestrin and ryanodine receptor in the heart, *Cell. Mol. Life Sci.* 70 (2013) 2935-2945.
- [39] J. Gaburjakova, M. Gaburjakova, Cardiac ryanodine receptor: Selectivity for alkaline earth metal cations points to the EF-hand nature of luminal binding sites, *Bioelectrochemistry* 109 (2016) 49-56.
- [40] P.P. Jones, W. Guo, S.R.W. Chen, Control of cardiac ryanodine receptor by sarcoplasmic reticulum luminal Ca^{2+} , *J. Gen. Physiol.* 149 (2017) 867-875.
- [41] J. Gaburjakova, M. Gaburjakova, Comparison of the effects exerted by luminal Ca^{2+} on the sensitivity of the cardiac ryanodine receptor to caffeine and cytosolic Ca^{2+} , *J. Membr. Biol.* 212 (2006) 17-28.
- [42] P.L. Diaz-Sylvester, M. Porta, J.A. Copello, Modulation of cardiac ryanodine receptor channels by alkaline earth cations, *PLoS One* 6 (2011) e26693.
- [43] B. Tencerova, A. Zahradnikova, J. Gaburjakova, M. Gaburjakova, Luminal Ca^{2+} controls activation of the cardiac ryanodine receptor by ATP, *J. Gen. Physiol.* 140 (2012) 93-108.
- [44] W. Guo, B. Sun, Z. Xiao, Y. Liu, Y. Wang, L. Zhang, R. Wang, S.R. Chen, The EF-hand Ca^{2+} binding domain is not required for cytosolic Ca^{2+} activation of the cardiac ryanodine receptor, *J. Biol. Chem.* 291 (2016) 2150-2160.
- [45] L.L. Ching, A.J. Williams, R. Sitsapesan, Evidence for Ca^{2+} activation and inactivation sites on the luminal side of the cardiac ryanodine receptor complex, *Circ. Res.* 87 (2000) 201-206.
- [46] M.D. Stern, Buffering of calcium in the vicinity of a channel pore, *Cell Calcium* 13 (1992) 183-192.
- [47] P. Petrovic, I. Valent, E. Cocherova, J. Pavelkova, A. Zahradnikova, Ryanodine receptor gating controls generation of diastolic calcium waves in cardiac myocytes, *J. Gen. Physiol.* 145 (2015) 489-511.
- [48] D. Jiang, B. Xiao, D. Yang, R. Wang, P. Choi, L. Zhang, H. Cheng, S.R. Chen, RyR2 mutations linked to ventricular tachycardia and sudden death reduce the threshold for store-overload-induced Ca^{2+} release (SOICR), *Proc. Natl. Acad. Sci. U. S. A.* 101 (2004) 13062-13067.
- [49] E. Nieboer, The lanthanide ions as structural probes in biological and model systems, *Structure and Bonding* 22 (1975) 1-47.
- [50] J.B. Lansman, Blockade of current through single calcium channels by trivalent lanthanide cations. Effect of ionic radius on the rates of ion entry and exit, *J. Gen. Physiol.* 95 (1990) 679-696.
- [51] L.M. Boland, T.A. Brown, R. Dingledine, Gadolinium block of calcium channels: influence of bicarbonate, *Brain Res.* 563 (1991) 142-150.

- [52] A.M. Beedle, J. Hamid, G.W. Zamponi, Inhibition of transiently expressed low- and high-voltage-activated calcium channels by trivalent metal cations, *J. Membr. Biol.* 187 (2002) 225-238.
- [53] S. Sarkozi, I. Komaromi, I. Jona, J. Almassy, Lanthanides report calcium sensor in the vestibule of ryanodine receptor, *Biophys. J.* 112 (2017) 2127-2137.
- [54] A. Malasics, D. Boda, M. Valiskó, D. Henderson, D. Gillespie, Simulations of calcium channel block by trivalent cations: Gd^{3+} competes with permeant ions for the selectivity filter, *Biochim. Biophys. Acta* 1798 (2010) 2013-2021.
- [55] D. Gillespie, M. Xu, G. Meissner, Selecting ions by size in a calcium channel: The ryanodine receptor case study, *Biophys. J.* 107 (2014) 2263-2273.
- [56] L. Lacinová, T-type calcium channel blockers - new and notable, *Gen. Physiol. Biophys.* 30 (2011) 403-409.
- [57] W. Liu, D.A. Pasek, G. Meissner, Modulation of Ca^{2+} -gated cardiac muscle Ca^{2+} -release channel (ryanodine receptor) by mono- and divalent ions, *Am. J. Physiol.* 274 (1998) C120-128.
- [58] H. Kong, P.P. Jones, A. Koop, L. Zhang, H.J. Duff, S.R. Wayne Chen, Caffeine induces Ca^{2+} release by reducing the threshold for luminal Ca^{2+} activation of the ryanodine receptor, *Biochem. J.* 414 (2008) 441-452.
- [59] M. Porta, A.V. Zima, A. Nani, P.L. Diaz-Sylvester, J.A. Copello, J. Ramos-Franco, L.A. Blatter, M. Fill, Single ryanodine receptor channel basis of caffeine's action on Ca^{2+} sparks, *Biophys. J.* 100 (2011) 931-938.
- [60] H.G. Brittain, F.S. Richardson, R.B. Martin, Terbium (III) emission as a probe of calcium (II) binding sites in proteins, *J. Am. Chem. Soc.* 98 (1976) 8255-8260.
- [61] E. Pidcock, G.R. Moore, Structural characteristics of protein binding sites for calcium and lanthanide ions, *J. Biol. Inorg. Chem.* 6 (2001) 479-489.
- [62] S.M. Simon, R.R. Llinas, Compartmentalization of the submembrane calcium activity during calcium influx and its significance in transmitter release, *Biophys. J.* 48 (1985) 485-498.
- [63] B. Dragani, A. Aceto, About the role of conserved amino acid residues in the calcium-binding site of proteins, *Arch. Biochem. Biophys.* 368 (1999) 211-213.
- [64] Y. Zhou, W. Yang, M. Kirberger, H.W. Lee, G. Ayalasomayajula, J.J. Yang, Prediction of EF-hand calcium-binding proteins and analysis of bacterial EF-hand proteins, *Proteins* 65 (2006) 643-655.
- [65] A. Fiser, R.K. Do, A. Sali, Modeling of loops in protein structures, *Protein Sci.* 9 (2000) 1753-1773.
- [66] D.A. Goldfeld, K. Zhu, T. Beuming, R.A. Friesner, Loop prediction for a GPCR homology model: algorithms and results, *Proteins* 81 (2013) 214-228.
- [67] J. Liou, M.L. Kim, W.D. Heo, J.T. Jones, J.W. Myers, J.E.J. Ferrell, T. Meyer, STIM is a Ca^{2+} sensor essential for Ca^{2+} -store-depletion-triggered Ca^{2+} influx, *Curr. Biol.* 15 (2005) 1235-1241.
- [68] J. Roos, P.J. DiGregorio, A.V. Yeromin, K. Ohlsen, M. Lioudyno, S. Zhang, O. Safrina, J.A. Kozak, S.L. Wagner, M.D. Cahalan, G. Velicelebi, K.A. Stauderman, STIM1, an essential and conserved component of store-operated Ca^{2+} channel function, *J. Cell Biol.* 169 (2005) 435-445.
- [69] Y. Huang, Y. Zhou, H.-C. Wong, Y. Chen, Y. Chen, S. Wang, A. Castiblanco, A. Liu, J.J. Yang, A single EF-hand isolated from STIM1 forms dimer in the absence and presence of Ca^{2+} , *FEBS J.* 276 (2009) 5589-5597.
- [70] S.R. Chen, L. Zhang, D.H. MacLennan, Characterization of a Ca^{2+} binding and regulatory site in the Ca^{2+} release channel (ryanodine receptor) of rabbit skeletal muscle sarcoplasmic reticulum, *J. Biol. Chem.* 267 (1992) 23318-23326.

- [71] Y. Hakamata, J. Nakai, H. Takeshima, K. Imoto, Primary structure and distribution of a novel ryanodine receptor/calcium release channel from rabbit brain, *FEBS Lett.* 312 (1992) 229-235.
- [72] W.E. Miranda, V.A. Ngo, R. Wang, L. Zhang, S.R. Chen Wayne, S.Y. Noskov, Molecular mechanism of conductance enhancement in narrow cation selective membrane channels, *J. Phys. Chem. Lett.* 9 (2018) 3497-3502.
- [73] D. Gillespie, L. Xu, Y. Wang, G. Meissner, (De)constructing the ryanodine receptor: modeling ion permeation and selectivity of the calcium release channel, *J. Phys. Chem. B* 109 (2005) 15598-15610.
- [74] T. Lu, A.Y. Ting, J. Mainland, L.Y. Jan, P.G. Schultz, J. Yang, Probing ion permeation and gating in a K^+ channel with backbone mutations in the selectivity filter, *Nat. Neurosci.* 4 (2001) 239-246.
- [75] R.A. Piskorowski, R.W. Aldrich, Relationship between pore occupancy and gating in BK potassium channels, *J. Gen. Physiol.* 127 (2006) 557-576.
- [76] S.G. Priori, C. Napolitano, N. Tiso, M. Memmi, G. Vignati, R. Bloise, V. Sorrentino, G.A. Danielli, Mutations in the cardiac ryanodine receptor gene (hRyR2) underlie catecholaminergic polymorphic ventricular tachycardia, *Circulation* 103 (2001) 196-200.
- [77] P.J. Laitinen, K.M. Brown, K. Piippo, H. Swan, J.M. Devaney, B. Brahmabhatt, E.A. Donarum, M. Marino, N. Tiso, M. Viitasalo, L. Toivonen, D.A. Stephan, K. Kontula, Mutations of the cardiac ryanodine receptor (RyR2) gene in familial polymorphic ventricular tachycardia, *Circulation* 103 (2001) 485-490.
- [78] A. Leenhardt, I. Denjoy, P. Guicheney, Catecholaminergic polymorphic ventricular tachycardia, *Circulation* 5 (2012) 1044-1052.
- [79] D.J. Tester, L.J. Kopplin, M.L. Will, M.J. Ackerman, Spectrum and prevalence of cardiac ryanodine receptor (RyR2) mutations in a cohort of unrelated patients referred explicitly for long QT syndrome genetic testing, *Heart Rhythm* 2 (2005) 1099-1105.
- [80] D.J. Tester, M. Dura, E. Carturan, S. Reiken, A. Wronska, A.R. Marks, M.J. Ackerman, A mechanism for sudden infant death syndrome (SIDS): stress-induced leak via ryanodine receptors, *Heart Rhythm* 4 (2007) 733-739.
- [81] D. Jiang, B. Xiao, L. Zhang, S.R. Wayne Chen, Enhanced basal activity of a cardiac Ca^{2+} release channel (ryanodine receptor) mutant associated with ventricular tachycardia and sudden death, *Circ. Res.* 91 (2002) 218-225.
- [82] D. Jiang, P.P. Jones, D.R. Davis, R. Gow, M.S. Green, D.H. Birnie, S.R. Chen, M.H. Gollob, Characterization of a novel mutation in the cardiac ryanodine receptor that results in catecholaminergic polymorphic ventricular tachycardia, *Channels (Austin)* 4 (2010) 302-310.

FIGURE LEGENDS

Schematic 1 Schematic representation of the experimental strategy. Luminal regulation of the RYR2 channel was studied in the presence of luminal Ca^{2+} or Ba^{2+} (M^{2+}). Luminally added Eu^{3+} competes with Ca^{2+} or Ba^{2+} for the luminal Ca^{2+} site, but does not have access to the cytosolic Ca^{2+} site because the RYR2 pore is completely blocked by Eu^{3+} .

Figure 1 Luminal Eu^{3+} permanently blocks the RYR2 current by total occlusion of the channel pore. RYR2 currents (upward deflections) recorded in the presence of luminal Eu^{3+} added to 8 mM $[\text{Ca}^{2+}]_{\text{L}}$ (A) or 8 mM $[\text{Ba}^{2+}]_{\text{L}}$ (B, top trace). A permanent total blockage of the Ba^{2+} current was transiently relieved by a negative potential (B, bottom trace). (C) Dependence of conductance (\circ, \bullet) and the current at 0 mV (Δ, \blacktriangle) on $[\text{Eu}^{3+}]_{\text{L}}$ when 8 mM $[\text{Ca}^{2+}]_{\text{L}}$ (\circ, Δ) or 8 mM $[\text{Ba}^{2+}]_{\text{L}}$ (\bullet, \blacktriangle) was present. Data shown are average \pm SEM ($N \geq 5$).

Figure 2 Luminal Eu^{3+} reduces RYR2 responsiveness to caffeine in the presence of 8 mM $[\text{Ca}^{2+}]_{\text{L}}$. (A) RYR2 currents (upward deflections) recorded before (control) and after 4 mM $[\text{Eu}^{3+}]_{\text{L}}$ was added. (B) Dependence of RYR2 P_O on caffeine concentration at 0 (\circ), 1 (\bullet), 2 (\ominus), 3 (Δ), and 4 mM $[\text{Eu}^{3+}]_{\text{L}}$ (\blacktriangle) (left). The caffeine EC_{50} values are plotted against $[\text{Eu}^{3+}]_{\text{L}}$ (right). Data shown are average \pm SEM (** $P < 0.01$, *** $P < 0.001$, vs. 0 mM $[\text{Eu}^{3+}]_{\text{L}}$, $N \geq 5$).

Figure 3 Luminal Eu^{3+} does not alter RYR2 gating in the presence of 8 mM $[\text{Ca}^{2+}]_{\text{L}}$. (A) RYR2 currents (upward deflections) illustrating channel gating at 0, 2, and 4 mM $[\text{Eu}^{3+}]_{\text{L}}$. RYR2 channels were activated by caffeine. (B) Dependence of F on P_O (left) obtained at 0 (\circ), 1 (\bullet), 2 (\ominus), 3 (Δ), and 4 mM $[\text{Eu}^{3+}]_{\text{L}}$ (\blacktriangle). Summary of the RYR2 F^{max} results displayed against $[\text{Eu}^{3+}]_{\text{L}}$ (right). Data shown are average \pm SEM ($N = 27$ for 0 mM $[\text{Eu}^{3+}]_{\text{L}}$ and $N \geq 5$ for other tested $[\text{Eu}^{3+}]_{\text{L}}$).

Figure 4 Cytosolic Ca^{2+} sensitivity of the RYR2 channel is not affected by luminal Eu^{3+} . Dependence of RYR2 P_O on $[\text{Ca}^{2+}]_{\text{C}}$ at 0 (\circ) and 4 mM $[\text{Eu}^{3+}]_{\text{L}}$ (\blacktriangle) (left). The values of EC_{50} for cytosolic Ca^{2+} are plotted against $[\text{Eu}^{3+}]_{\text{L}}$ (right). Data shown are average \pm SEM ($N \geq 5$).

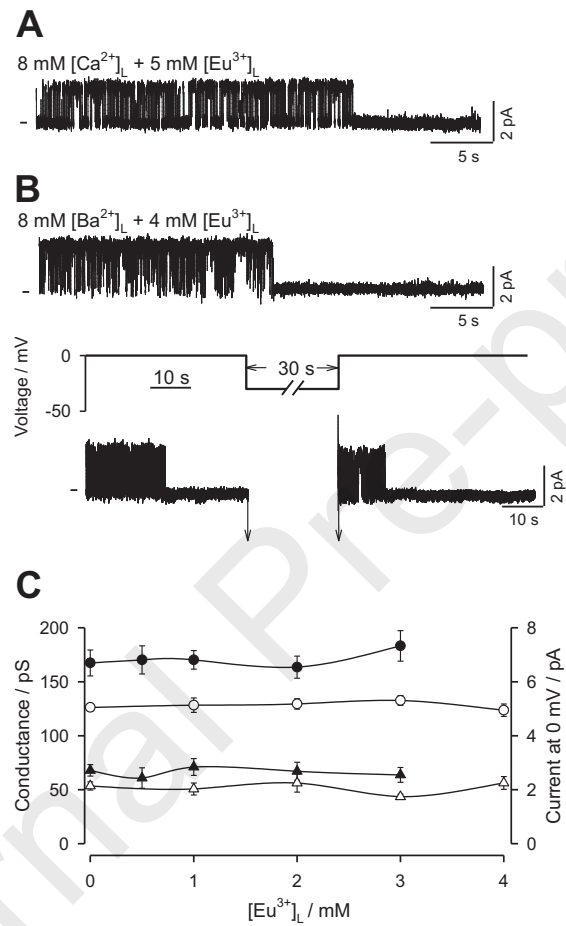
Figure 5 Luminal Eu^{3+} has no appreciable effect on caffeine-dependent RYR2 activation in the presence of 8 mM $[\text{Ba}^{2+}]_{\text{L}}$. (A) RYR2 currents (upward deflections) recorded before (control) and after addition of 3 mM $[\text{Eu}^{3+}]_{\text{L}}$. (B) Dependence of RYR2 P_O on caffeine concentration at 0 (\circ), 0.5 (\bullet), 1 (\ominus), 2 (Δ), and 3 mM $[\text{Eu}^{3+}]_{\text{L}}$ (\blacktriangle) (left). The caffeine EC_{50} values are plotted against $[\text{Eu}^{3+}]_{\text{L}}$ (right). Data shown are average \pm SEM ($N = 24$ for 0 mM $[\text{Eu}^{3+}]_{\text{L}}$ and $N \geq 5$ for other tested $[\text{Eu}^{3+}]_{\text{L}}$).

Figure 6 Luminal Eu^{3+} does not modulate RYR2 gating in the presence of 8 mM $[\text{Ba}^{2+}]_{\text{L}}$. (A) RYR2 currents (upward deflections) acquired at 0, 1, and 3 mM $[\text{Eu}^{3+}]_{\text{L}}$. RYR2 channels were activated by caffeine. (B) The P_O -dependence of RYR2 F (left) obtained at 0 (\circ), 0.5 (\bullet), 1 (\ominus), 2 (Δ), and 3 mM $[\text{Eu}^{3+}]_{\text{L}}$ (\blacktriangle). The values of RYR2 F^{max} displayed against $[\text{Eu}^{3+}]_{\text{L}}$ (right). Data shown are average \pm SEM ($N = 24$ for 0 mM $[\text{Eu}^{3+}]_{\text{L}}$ and $N \geq 5$ for other tested $[\text{Eu}^{3+}]_{\text{L}}$).

Figure 7 Effects of $\text{Eu}^{3+}/\text{Ca}^{2+}$ versus $\text{Eu}^{3+}/\text{Ba}^{2+}$ competition on the RYR2 luminal face. Data replotted from Figs. 2B, 3B, 5B and 6B. (A) The addition of 4 mM $[\text{Eu}^{3+}]_{\text{L}}$ to 8 mM $[\text{Ca}^{2+}]_{\text{L}}$ shifted the caffeine dose-response curve to the right (short dashed line).

Adding 3 mM $[\text{Eu}^{3+}]_{\text{L}}$ to 8 mM $[\text{Ba}^{2+}]_{\text{L}}$ caused only a negligible shift to the left (long dashed line). RYR2 responsiveness to caffeine is likely controlled by a luminal-facing Ca^{2+} site (right panel). **(B)** Adding 4 mM $[\text{Eu}^{3+}]_{\text{L}}$ to 8 mM $[\text{Ca}^{2+}]_{\text{L}}$ (short dashed line) or 3 mM $[\text{Eu}^{3+}]_{\text{L}}$ to 8 mM $[\text{Ba}^{2+}]_{\text{L}}$ (long dashed line) did not cause any vertical shift in the P_{O} -dependence of F . RYR2 gating behavior is presumably regulated inside the channel pore (right panel).

Figure 8 Comparison of effects induced by Eu^{3+} and alkaline earth metal cations (M^{2+}) on the RYR2 luminal face in the presence of luminal Ca^{2+} . The caffeine EC_{50} (**A**) and F^{max} values (**B**) displayed as a function of $[\text{Eu}^{3+}]_{\text{L}}/8 \text{ mM } [\text{Ca}^{2+}]_{\text{L}}$ (\circ , data taken from Figs. 2B and 3B) and $[\text{M}^{2+}]_{\text{L}}/1 \text{ mM } [\text{Ca}^{2+}]_{\text{L}}$ (M^{2+} : $\text{Sr}^{2+} \bullet$, $\text{Mg}^{2+} \ominus$, and $\text{Ba}^{2+} \Delta$, data taken from [39]). Also shown are the caffeine EC_{50} and F^{max} values for pure 1 mM $[\text{Ca}^{2+}]_{\text{L}}$ (dash-dot-dotted line), 8 mM $[\text{Ca}^{2+}]_{\text{L}}$ (solid line), and 8–53 mM $[\text{M}^{2+}]_{\text{L}}$ (Sr^{2+} dotted line, Mg^{2+} dash-dotted line, and Ba^{2+} dashed line). Data shown are average \pm SEM.

**FIGURE 1** (1 column fitting)

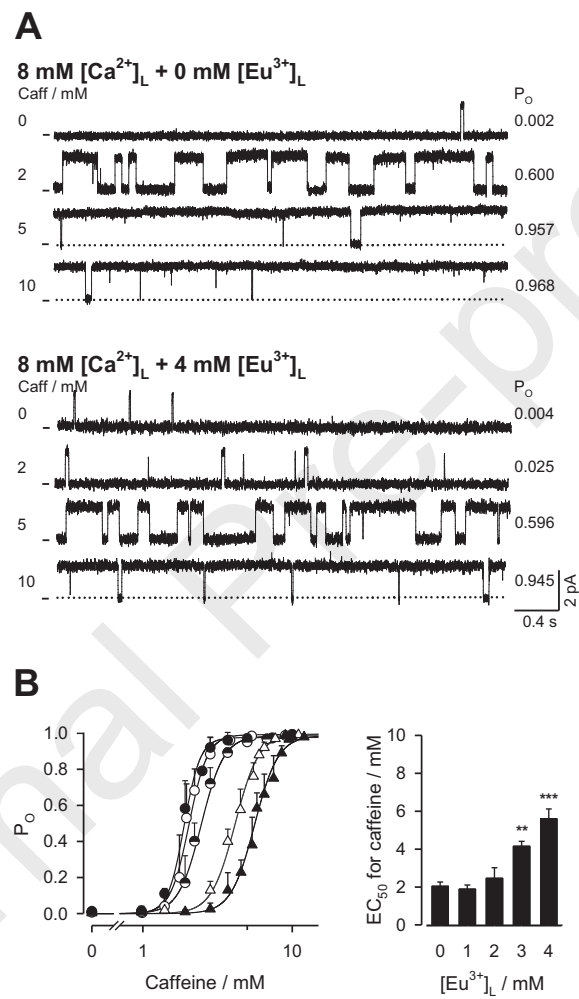


FIGURE 2 (1 column fitting)

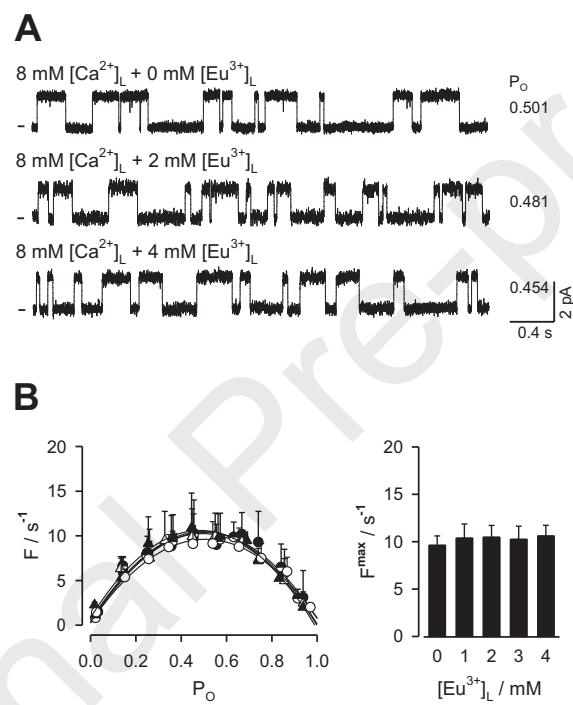


FIGURE 3 (1 column fitting)

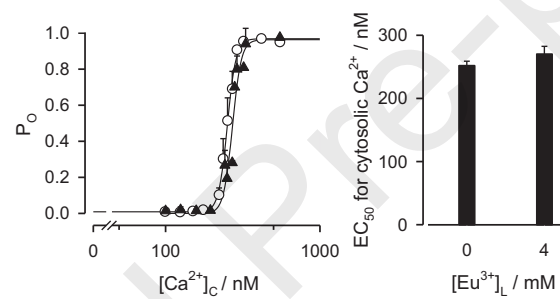
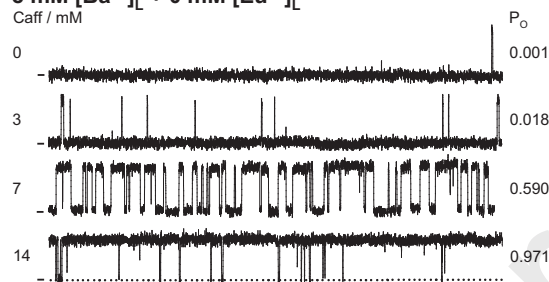
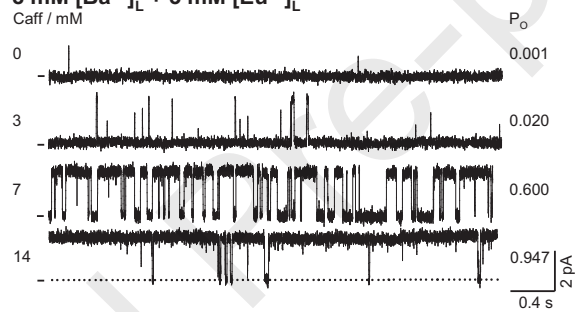
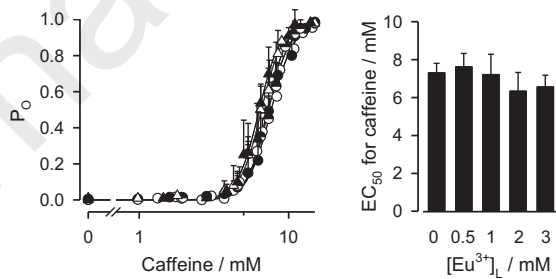


FIGURE 4 (1 column fitting)

A**8 mM [Ba²⁺]_L + 0 mM [Eu³⁺]_L****8 mM [Ba²⁺]_L + 3 mM [Eu³⁺]_L****B****FIGURE 5** (1 column fitting)

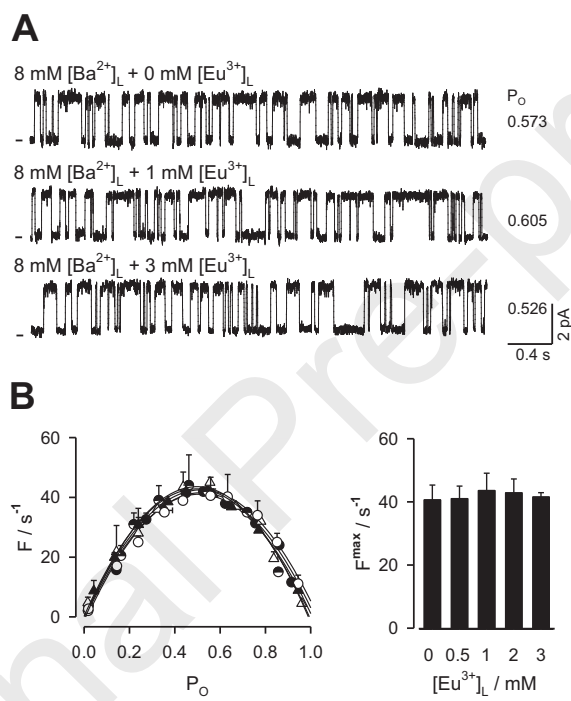
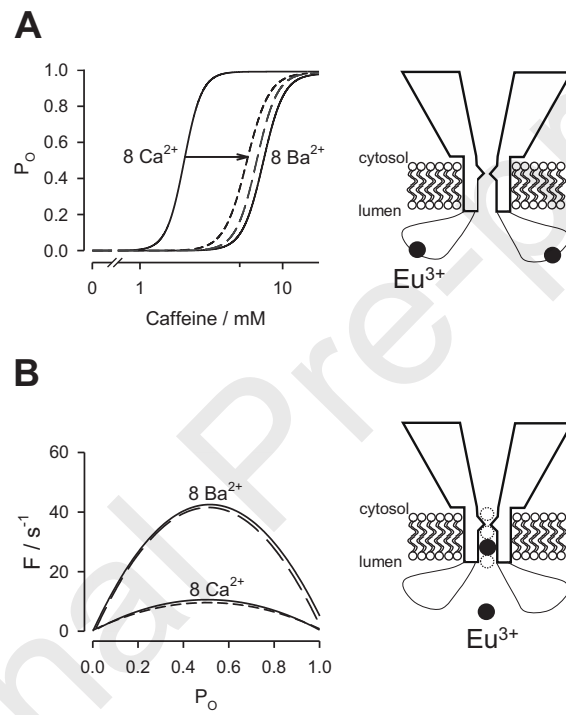
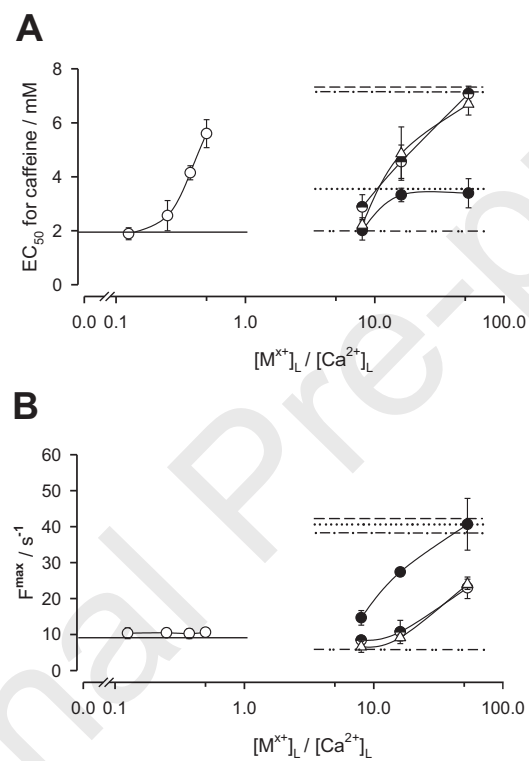
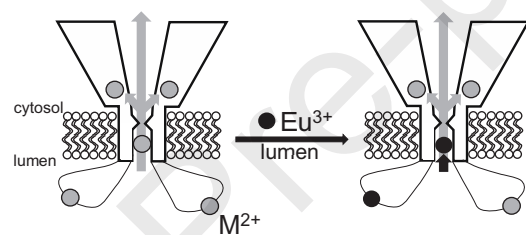


FIGURE 6 (1 column fitting)

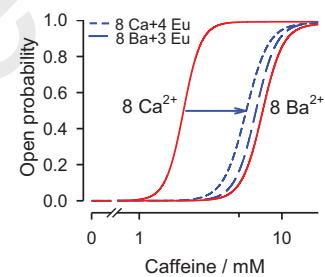
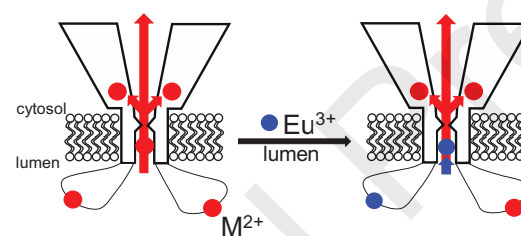
**FIGURE 7** (1 column fitting)

**FIGURE 8** (1 column fitting)



SCHEMATIC 1 (1 column fitting)

RyR2 channel



Highlights

- Non-permeant luminal Eu^{3+} interacts with RYR2 Ca^{2+} sites accommodating luminal Ca^{2+} .
- Luminal Ca^{2+} -mediated RYR2 response to caffeine is antagonized by luminal Eu^{3+} .
- Gating behavior of the RYR2 channel is insensitive to luminal Eu^{3+} .
- RYR2 responsiveness to caffeine is likely controlled by a luminal-facing Ca^{2+} site.
- RYR2 gating behavior is presumably regulated inside the channel pore.

Declaration of interests

☒ The authors declare that they have no known competing financial interests or personal relationships that could have appeared to influence the work reported in this paper.

☐ The authors declare the following financial interests/personal relationships which may be considered as potential competing interests:

--